**Turkish Journal of FISHERIES and AQUATIC SCIENCES**

RESEARCH PAPER

# Morphological and Molecular Characterization of Neritic Zooplankton in Marguerite Bay, Antarctica

**Alpaslan Kara² ⓘ, Tuba Terbıyık Kurt³ ⓘ, Meral Apaydin Yağci² ⓘ, Erdinç Veske⁴ ⓘ, Engin Kocabaş² ⓘ, Haşim İnceoğlu² ⓘ, Murat Keleş² ⓘ, Ramazan Aymaz² ⓘ, Yalçın Yaman¹,\* ⓘ**

¹Siirt Universitiy, Faculty of Veterinary Medicine, Department of Genetics, Siirt, TÜRKİYE.
²Sheep Breeding and Research Institute, Bandırma, Balıkesir, TÜRKİYE.
³Çukurova University, Faculty of Fisheries, Marine Biology, Adana, TÜRKİYE.
⁴Republic of Türkiye Ministry of Agriculture and Forestry General Directorate of Agricultural Research and Policies, Ankara, TÜRKİYE.

**How to Cite**

**Abstract**

This study details field investigations conducted during the 6th Turkish National Antarctic Science Expedition in February 2022, involving zooplankton sampling at ten stations along the western shores of Horseshoe Island, Marguerite Bay. Utilizing a WP-2 plankton net, both vertical and horizontal sampling methods were employed, with samples preserved for morphological and molecular analysis. Morphological assessments of collected zooplankton focused on detailed descriptions supported by digital imaging. Following Antarctic marine fieldwork, genetic research was initiated with DNA extraction from zooplankton specimens. Molecular analyses focused on amplifying mitochondrial gene regions. These mitochondrial DNA markers are recognized for species identification and phylogenetic investigations. This study was conducted by combining classical morphological assessment with mitochondrial DNA barcoding technology. As a result, molecular analyses of *Calanoides acutus* and *Paralabidocera grandispina* revealed high identity percentages (≥98%) when compared to reference sequences in the BOLD database, demonstrating successful species identification through mitochondrial DNA (mtDNA) barcoding. Detailed morphological features of these two species, as well as others, were documented with particular focus on the structure of the swimming legs and genital segments. The study aims to contribute to the understanding of zooplankton biodiversity in Antarctic marine ecosystems, providing preliminary insights into genetic diversity and potential cryptic species through molecular genetic techniques.

## Introduction

Zooplankton are a critical component of marine ecosystems, serving as an important pathway for energy transfer between primary producers and higher trophic levels such as fish, seabirds, and marine mammals (Heneghan et al., 2016). They also influence oceanic biogeochemical cycles through direct and indirect feedback loops (Ratnarajah et al., 2023). Recycling by zooplankton drives the cycling of essential micronutrients in the upper ocean (Richon et al., 2021). Both biotic and abiotic factors influence the dynamics of aquatic biota, making ecosystems and inhabitants, like zooplankton, particularly vulnerable to climate change. Significant consequences include rising temperatures, acidification, nutrient enrichment, and heightened ultraviolet (UV) exposure, all of which adversely impact zooplankton survival, behaviour, nutrition, reproduction, and overall population dynamics (Arafat et al., 2021).

Antarctica is considered the most sensitive region to global climate change due to its unique geographical location and ecology (Cheng et al., 2013). Global surface air temperature records show a warming of 5–6 °C during winter over the last 50 years, and with the projected global temperature increase of at least 1–3 °C in the coming century, Antarctic ecosystems are likely to experience further warming and glacial melting (Hernando et al., 2020). Within the broader global temperature increase trend, the warming of the Antarctic Peninsula is particularly notable (Ducklow, 2007). Significant changes have occurred in the Southern Ocean over the past half-century, as revealed through instrument records, station observations, satellite data, and paleoenvironmental records (Bax et al., 2021). The climate is changing more rapidly in western Antarctica, with temperatures increasing since 1950 (Lee et al., 2017).

Environmental factors such as temperature, salinity, and especially sea ice cover significantly influence the characteristics of zooplankton community structure in Antarctica (Yang et al., 2011; Ward et al., 2004). This trend is particularly pronounced in the western Antarctic Peninsula, where a 40% reduction in sea ice has been observed from 1979 to the present (Montes-Hugo et al., 2010).

Zooplankton identification has long been hindered by significant morphological challenges, a limitation widely recognized in marine biological research (Bucklin et al., 2011). Marine copepods, which are critical constituents of oceanic ecosystems, exemplify these taxonomic difficulties. Their remarkably similar morphological structures make species differentiation exceptionally complex (Blanco-Bercial et al., 2014).

The persistent challenge lies in distinguishing between species that appear virtually identical under conventional microscopic examination, necessitating new approaches to unravel the intricate biodiversity within these crucial marine microorganisms. DNA barcoding emerged as a prominent molecular approach with the proposal of the cytochrome c oxidase I (COI) gene as a standardized target for animal species identification in 2003 (Hebert et al., 2003). This method enables rapid and precise species identification through the utilization of standardized short DNA segments, representing a significant advancement in molecular taxonomic techniques (Hebert and Gregory, 2005). The methodology serves two fundamental scientific objectives: distinguishing species at the DNA level and facilitating the discovery of novel taxonomic entities through genetic information (DeSalle et al., 2005). Critically, DNA barcoding is not intended to invalidate or replace traditional morphological taxonomic classification, but rather to complement existing systematic approaches (Bucklin et al., 2011).

The purpose of the study is to enhance the understanding of zooplankton biodiversity in the Southern Ocean, particularly in Antarctic marine ecosystems, by integrating traditional morphological species identification methods with DNA barcoding technology. While classical morphological approaches have long been used for species identification, they often face challenges due to the high variability and complexity of some zooplankton species. By incorporating DNA barcoding, specifically mitochondrial DNA markers such as cytochrome c oxidase subunit I (COI), this study aims to overcome these limitations and provide more accurate and reliable species identification. This combined approach not only strengthens the accuracy of morphological assessments but also offers a powerful tool for discovering potential cryptic species and gaining insights into the genetic diversity of zooplankton populations in the Southern Ocean.

## Materials and Methods

Field studies were conducted in February 2022 at 10 stations (Figure 1) as part of the 6th Turkish National Antarctic Science Expedition.

Plankton samples were collected using a WP-2 plankton net with a 57 cm mouth opening and 300 μm mesh size from the western shores of Horseshoe Island, facing Marguerite Bay. Sampling was conducted vertically and horizontally for 10 minutes each, using rigid boats. Vertical tows were taken from 4 meters above the seafloor, while horizontal tows involved positioning the plankton net below the water surface and retrieving it promptly after the 10-minute interval. Collected samples were preserved in 330 ml containers. Zooplankton were sorted the same day under a microscope. The morphological descriptions of zooplankton aim to detail all visible characteristics and are supported by photographs.

For DNA extraction, the samples were first washed in sterile distilled water to remove ethanol. Commercial spin-column kits (DNeasy Blood and Tissue Kits, Valencia, CA, USA) were used, following the manufacturer's protocol with some modifications, such as increased protease K and overnight incubation to improve DNA purity. The extracted DNA was stored at -20°C until PCR analysis.

Primers targeting the mitochondrial COI, reported by Bucklin et al. (2010) and Cheng et al. (2013) were used to perform PCR. PCR products were analyzed on 1.2-2% agarose gels to assess band quality. Samples with high-quality bands on electrophoresis were sequenced using the Sanger method. Sequence analyses were conducted on an ABI 3500 platform at the Sheep Breeding Research Institute's Molecular Genetics laboratories. For sequencing, 2.5-4 μl of each sample was taken for preliminary purification. Exo-SAP enzyme was used at 37°C for 30 minutes, followed by denaturation at 85°C for 15 minutes. The chain termination reaction was then performed using the BigDye Terminator v3.1 Cycle Sequencing Kit. Final purification was conducted using the ethanol precipitation method, after which the products were
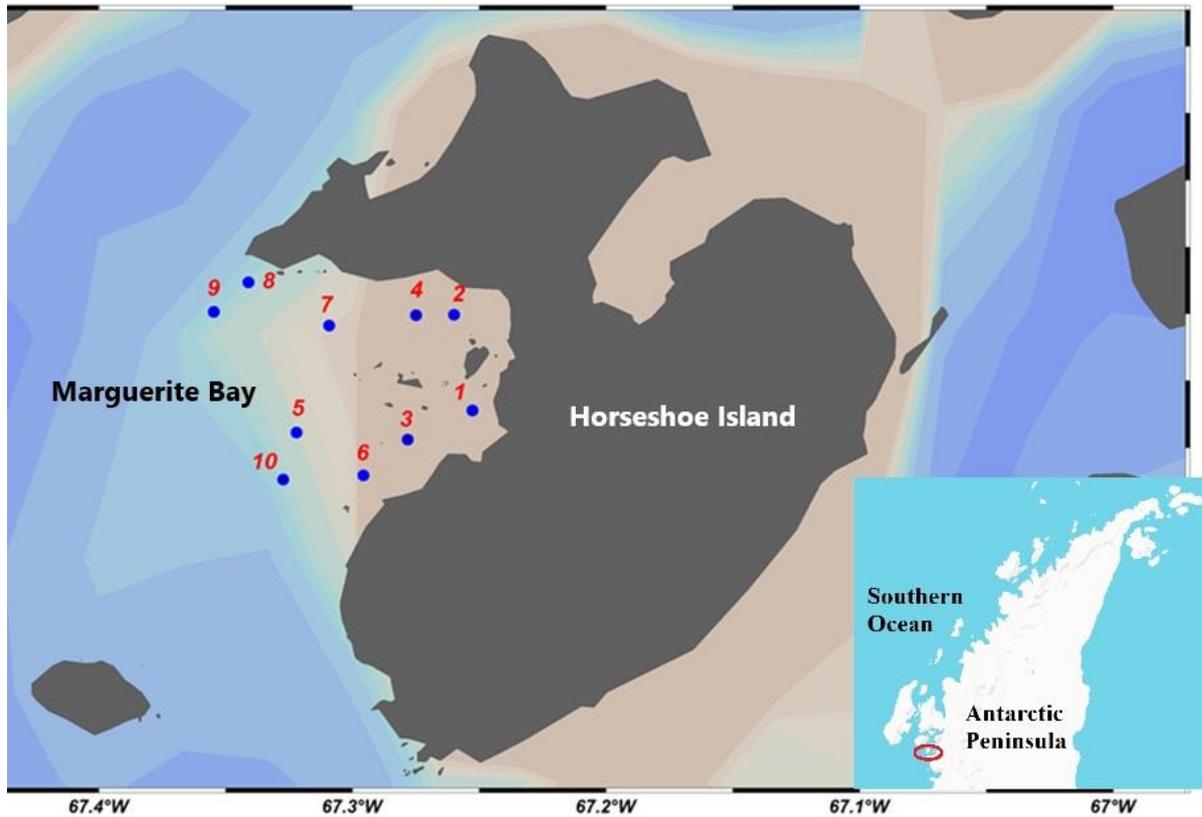
**Figure 1.** Sampling stations.

treated with formamide and subjected to capillary electrophoresis on the ABI 3500 platform under appropriate parameters. Chromatogram files were visualised using FinchTV (Geospiza Inc., Seattle, WA, USA). Forward and reverse reads were aligned in Mega7 (Kumar et al., 2016), with errors corrected using both sequence data and chromatogram peaks. Edited barcodes were compared with barcode sequences in the databases using the BLAST tools from the BOLD system (https://boldsystems.org/) and NCBI (https://blast.ncbi.nlm.nih.gov/Blast.cgi), to verify nucleotide similarities with matching species.

## Results

### DNA Barcoding

The targeted species, identity results, and BOLD system IDs for the species identified through DNA barcoding are as follows:

| Targed species | Primer Fw | Primer Rv-1 | Primer Rv-2 | Primer references | Identity (%) | BOLD system ID |
|---|---|---|---|---|---|---|
| *Calanoides acutus* | Coxf | Coxr1 | Coxr2 | Cheng et al. (2013) | ≥ 98 | TRKY002-22 |
| *Paralabidocera grandispina* | cop-COI-1498 | cop-COI-2198R | - | Bucklin et al. (2010) | ≥ 98 | TRKY003-22 |

Mitochondrial DNA (mtDNA) barcoding techniques revealed remarkably high nucleotide similarities (≥ 98%) among target species. Existing research indicates that while variations exist between species, nucleotide differences up to 3% between reference genomes and sample barcode sequences may potentially represent intraspecific diversity (Chakraborty and Ghosh, 2014). Consequently, the observed nucleotide variations ≤2% between barcoded samples and their respective reference genomes were considered within acceptable limits for species identification using mtDNA barcoding methodology.

Despite morphological identification of target species, including Oithona sp. and four Ctenocalanus sp., successful PCR amplification was challenging and ultimately unsuccessful for these taxa, precluding their molecular barcoding. In addition to the primer pairs initially presented in the primer table, alternative zooplankton primers reported by Folmer et al. (1994), Machida et al. (2004), Goodall-Copestake et al. (2010), and Geller et al. (2013) were systematically tested, yet failed to yield interpretable genetic results. We hypothesize that extensive marine transit and prolonged sample storage likely induced significant DNA degradation, compromising the molecular integrity of these specimens. Such degradation can substantially impede genetic amplification, particularly in marine organisms subjected to extended environmental and logistical challenges during research expeditions.

### Morphological Characterization

During the 6th Turkish National Antarctic Science Expedition, the collected specimens included *Calanoides acutus* (1 female), *Parablennius grandispinna* (14

females, 13 males), *Oithona frigida* (1 female), and *Oithona smilis* (7 females). The morphological examination strategy and results were as follows:

### *Calanoides acutus* (Giesbrecht, 1902) ♀

All individuals were initially identified at the group level, and their counts were recorded. Adult individuals belonging to the Copepoda family were identified as accurately as possible at the species level. Morphological characterizations were performed solely on adult individuals. However, samples preserved in ethanol did not yield optimal results for morphological examination, as body integrity was not maintained in nearly all individuals, limiting morphological characterisation. In some species, only a single individual was observed, and as the same sample was also used for molecular characterisation, detailed dissection could not be performed. Species identifications were conducted using an Olympus BX 50 light microscope, with photographs taken using a Nikon D7200 camera mounted on the microscope. Total body length was measured from the anterior end of the prosome to the distal end of the caudal ramus, prosome length from the anterior end of the prosome to the distal end of the last segment, and urosome length from the beginning of the first segment of the urosome to the distal end of the caudal ramus.

Only one individual of this species was observed. The structure of the fifth leg is crucial for identifying Calanoides species, but due to broken segments of the fifth leg (P5) of the available individual, species identification could not be performed.

The total length is 2.2 mm. The body is torpedo-shaped, long, and slender (Figure 2a). The prosome widens gradually from the head towards the middle of the body, then narrows again towards the posterior end. The lower edge of the prosome is not pointed but narrows towards the tip (Figure 2a). In lateral view, it appears rounded (Figure 2b). The head appears slightly triangular from a dorsal view (Figure 2a) and descends triangularly towards the front in lateral view (Figure 2b). The prosome carries two filament-like rostrums that droop downwards (Figure 2c). The ratio of total body length to prosome length is measured as 0.8, with the Pr/Ur ratio at 4 and the Cr/Pr ratio at 0.375. The ratio of the prosome segments is measured as 150:82:52:45:33:38. The urosome consists of four segments and the caudal rami (Figure 2a,b). The ratio of the urosome segments and caudal rami is 36:33:15:11:19. The genital segment appears slightly swollen from the dorsal view, tapering slightly towards the lower end to match the thickness of the other urosome segments. The urosome segments also taper slightly towards the anal segment. The caudal rami bear six setae, one of which is short and thin, while the others are thick and long (Figure 2d). The length-to-width ratio is approximately 1.9.

A1 has 25 segments and extends about one segment beyond the distal end of the caudal rami (Figure 2b). Several stout, seta-like structures are present at the tip of the outermost segment. Each segment has small hairs. A2 is bifurcated, with well-developed coxa and basis (Figure 2e). The exopodite has seven segments, with long setae on each segment (Figure 2e). The endopodite consists of two segments, with two long setae near the edge where it joins the basis. The distal end of End2 is divided into two lobes, with nine setae on the inner lobe and seven on the outer lobe (Figure 2e). The mandible is well-developed (Figure 2f), with four long setae on the basis. Enp1 carries four long setae on its outer edge, while Enp2 has 11 setae. The exopod has five segments and carries six long setae. Long setae are also present on the edge of the basipod (Figure 2f). Mx1l is well-developed, with distinct segments (Figure 2g). Le2 contains one seta (Figure 2g). In Mx2, the endites and endopodite are visible, each bearing long setae (Figure 2h). The maxilliped is fully developed, of normal structure, and consists of seven segments (Figure 2i), with long setae on all segments.

All swimming legs are bifurcated, with three-segmented exopodites and endopodites (Figure 2j,k,l,m). In the first leg, the distal seta on the inner side of the basis is curved and extends inward (Figure 2j). Detailed characterization could not be performed for P5 due to broken exopod segments. The inner edge of the P5 coxa is not serrated (Figure 2n).

### *Paralabidocera grandispina* Waghorn, 1979 ♀

Four female individuals of *Paralabidocera grandispina* were sampled. The total length is 1.68 mm, and the body is long and oval in shape (Figure 3a), with the head clearly separated from the first body segment. The fourth and fifth body segments are fused (Figure 3a). The prosome is longer than the urosome, with a Pr/Ur ratio of approximately 2.47. The posterior end of the prosome has a blunt triangular projection (Figure 4a). The urosome consists of three segments (Figure 4a); however, specific segment ratios are indistinct due to deformation.

A1 is shorter than the prosome and only reaches the end of the first body segment, with segments bearing long setae (Figure 3b). The maxillule, maxilla, and mandible are deformed and could not be dissected or examined in detail.

The genital segment is relatively large, swollen, and asymmetrical, with various protrusions on both the right and left sides (Figure 3c). The subsequent urosome segments narrow abruptly (Figure 3c). The caudal rami are asymmetrical, with the right side slightly longer and wider. The caudal ramus has a width-to-length ratio of approximately 2.1 (Figure 3d).

In legs P1 to P4, the exopodite is three-segmented, and the endopodite is two-segmented (Figures 3e, 3f, 3g). No clear boundary exists between the spines on the
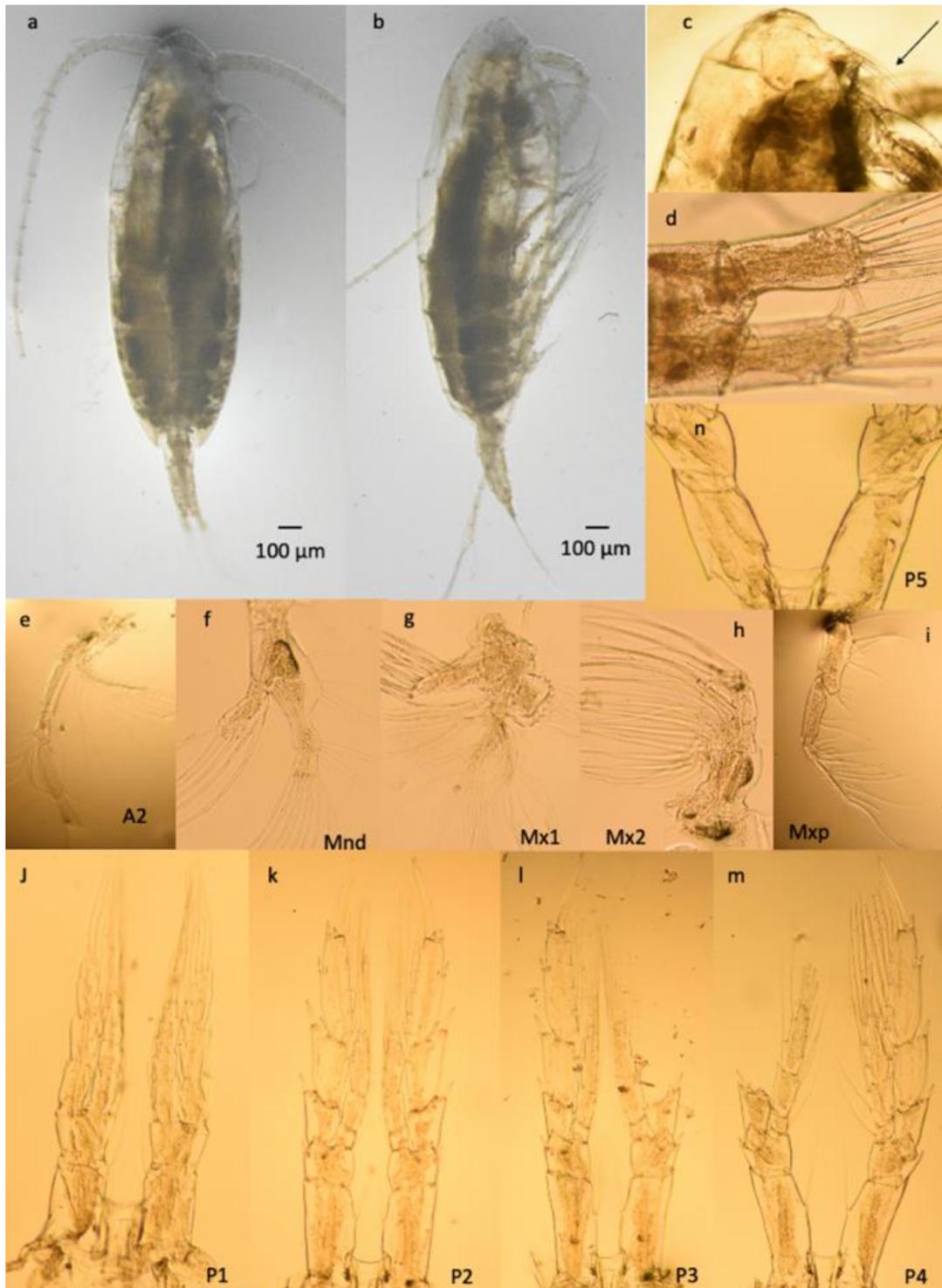
**Figure 2.** *Calanoides acutus*. a: Dorsal view of the entire body and urosome, b: Lateral view of the entire body, A1, c: Rostrum, d: Caudal rami, e: A2, f: Mandible (Mnd), g: Maxilla 1 (Mx1), h: Maxilla 2 (Mx2), i: Maxilliped (Mxp), j: P1, k: P2, l: P3, m: P4, n: P5.

outer side of the exopod of legs P2 to P4 and the segments themselves (Figures 3e, 3f, 3g).

P5 is distinctly different from the other legs. The endopodite and exopodite are poorly developed (Figure 3h). The endopodite is reduced to a single, small, triangular segment (Figure 4h), while the exopod is one-segmented and elongated, with three parts: one large and two small branches. There is a thin, small hair between two of these branches (Figure 3h).

### *Paralabidocera grandispina* Waghorn, 1979 ♂

The total length is 1.38 mm. As in the female, the first thoracic segment is clearly separated from the head, and the fourth and fifth segments are fused (Figures 3i, 3j). The prosome is longer than the urosome, with a Pr/Ur ratio of 1.95. Unlike the female, the lower ends of the prosome are rounded and lack protrusions (Figures 3i, 3j). The urosome consists of five segments,
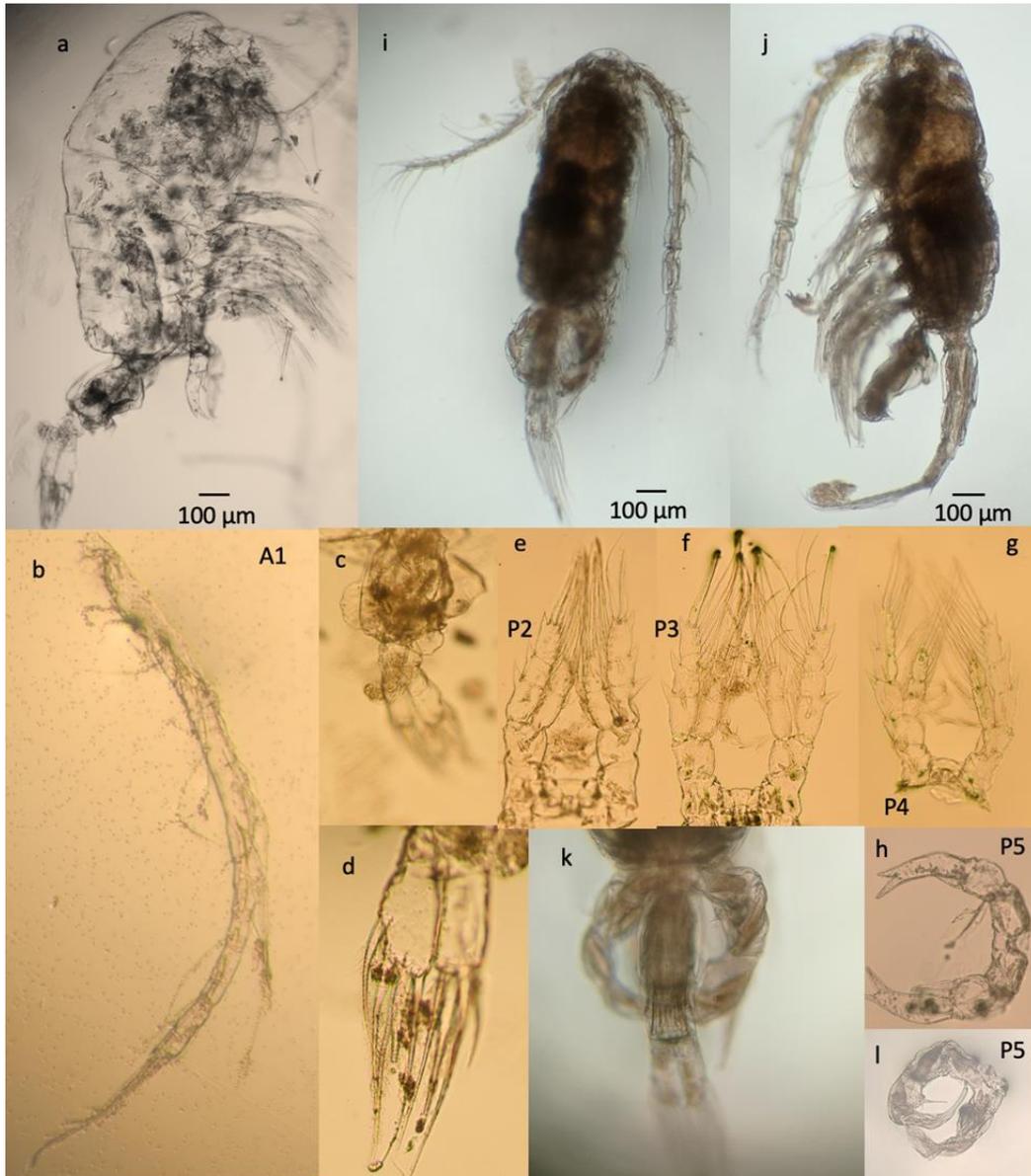
**Figure 3.** *Paralabidocera grandispina.* (♀), All lateral view b: A1, c: Urosome, d: Caudal rami, e: P2, f: P3, g: P4, h: P5, *Paralabidocera antarctica* (♂) i: Entire body dorsal view, j: Entire body lateral view, k: Urosome (♂), l: P5"P5.

with the segment and caudal rami ratios at 8:18:10:5:4:12 (Figure 3k). The genital segment is slightly widened distally, and the caudal rami are asymmetrical, with a length-to-width ratio of 2.1 (Figure 3k).

On the right side, A1 is geniculate, forming a grasping organ (Figure 3j). All legs except P5 resemble those in the female.

P5 is highly developed and complex (Figure 3l). On the right side, there are four segments attached to the basipod, as well as a poorly developed endopod. The second segment has a triangular projection on the inner side's centre. The terminal segment extends into a long whip-like shape. On the left side, there are three segments, with the first segment rounded and bearing small teeth on the inner side of the distal part. The third segment bends inward, tapering towards the end and carrying various setae and spines (Figure 3l).

### *Oithona frigida* Giesbrecht, 1902 ♀

The total length is measured at 1.05 mm. The prosome is torpedo-shaped (Figure 4a) and longer than the urosome, with a Pr/Ur ratio of 1.29. The prosome's length-to-width ratio is 2.5. The head tapers forward, and the rostrum appears pointed in a dorsal view (Figure 4a). In lateral view, the rostrum curves and narrows toward the tip (Figures 4a, b). The ratios of the urosome segments and the caudal rami are 14, 35, 20, 19, 16, and 12, respectively. The caudal rami length-to-width ratio is 2.67. The genital segment is widened in its first third, narrowing thereafter (Figure 4a). A1 and A2 are single-branched (Figures 4a, b), but both A1 pairs are broken in the specimen, so numerical values could not be measured. A2 has few, short segments (Figure 4b).

The mandible has two relatively long, spinulose spines on the basipod, with the inner spine being slightly
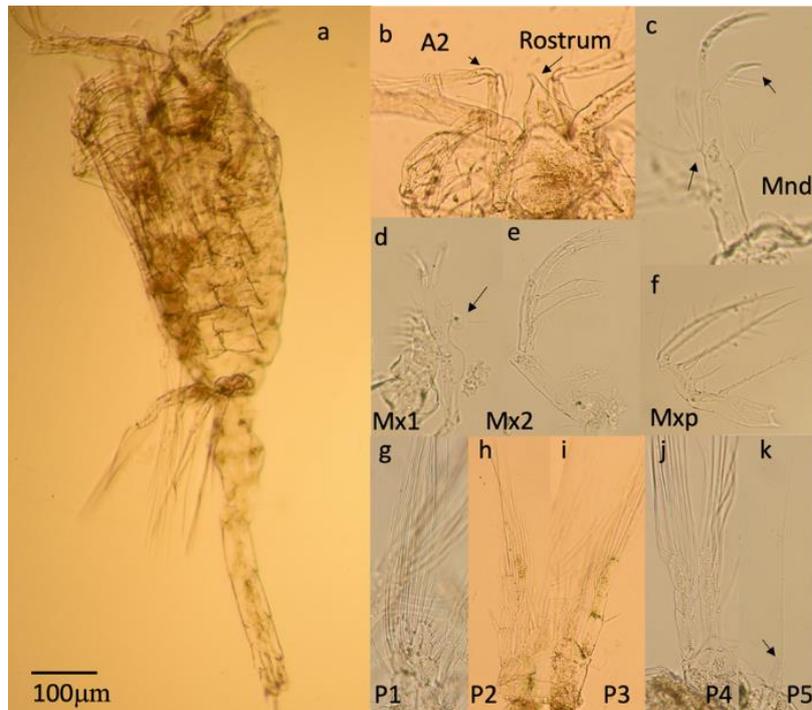
**Figure 4.** *Oithona frigida*. a: Entire ventral view, b: Head and A2 with rostrum, c: Mnd, d: Mx1, e: Mx2, f: Mxp, g: P1, h: P2, i: P3, j: P4, k: P5.

shorter. The endopodite carries four setae (Figure 4c). Mx1 has three thin, equal-length setae at the tip. Le1 and Li2 each have one seta, while Li3 has one thin, spinulose seta, one long seta, and one thick seta. The endopodite is oval and has one long seta of its own. The exopod has three setae (Figure 4d). Mx2 has two long, equal setae on the endopodite (Figure 5e). Due to damage, a complete morphological description of the maxilliped was not possible. End2 carries two equal-length spinulose setae, one short seta, and one small seta (Figure 4f).

The first four swimming legs are two-branched and similar in structure (Figures 4g, h, i, j). Each leg from P1 to P4 has three segments in both the endopod and exopod (Figures 4g, h, i, j). The fifth leg is reduced to a single seta, with a small seta at the distal end (Figure 4h).

### *Oithona similis* Claus, 1866 - Group ♀

The total length varies between 0.94 and 1.06 mm. The prosome is long and fusiform, comprising five segments (Figure 5a). In dorsal view, the head appears blunt as the rostrum is not visible from the front (Figure 5a), but in lateral view, the rostrum extends forward at a steep angle with a pointed structure (Figure 5b). The first three body segments have a similar thickness longitudinally, though they narrow laterally from the third segment toward the urosome, with the final segment being narrower and rounded at the ends.

The prosome is slightly longer than the urosome (Figure 5a), with a length-to-width ratio of 2.7. The Pr/Ur ratio ranges from 1.2 to 1.28. The urosome comprises five segments (Figure 5a). Ratios of the urosome

segments and the caudal rami are 11, 31, 13, 15, 13, and 11, respectively. The caudal rami length-to-width ratio is 2.2.

A1 is relatively long, extending slightly beyond the prosome (Figure 5b) and covered with numerous setae. A2 is single-branched and short (Figure 5c). The mandible has two pointed, slightly curved hairy spines at the distal end of the basipod (Figure 5d), with one seta on the inner side near the middle. The endopod has three setae (Figure 5d). Mx1 has a small, oval endopod without setae, while the exopod has three setae (Figure 5e). Due to damage, other morphological details could not be fully observed in the examined specimen. Mx2 has two long spinulose setae, one short thick seta, and one small seta (Figure 5f). The maxilliped has a few short, distinct setae along the inner edge of the basipod and shorter setae arranged distally on the front face (Figure 5g). End2 has two unequal long setae, one short seta, and one small seta (Figure 5g). The first four swimming legs are two-branched and similar in structure, each with three segments in both the endopod and exopod (Figure 5h, i, j, k). The fifth leg is reduced to a single seta (Figure 5l).

### Discussion

Molecular analyses of the genus *Calanoides* have identified only the species *C. acutus*. For morphological examinations, only one adult individual of this genus was available. Morphological studies of this individual were conducted in ethanol, and after the examination, it was re-tubed for preservation and future molecular characterisation. However, DNA could not be directly

**Figure 4.** *Oithona similis* group. a: Whole body dorsal view, A1 and urosome; b: Whole body lateral view and rostrum; c: A2; d: Mnd; e: Mx1; f: Mx2; g: Mxp; h: P1; i: P2; j: P3; k: P4; l: P5.

isolated from this individual. The results of the molecular analyses were obtained from copepodites of the *Calanoides* genus found at various stations. *Calanoides* can be easily distinguished from *Calanus* species by the absence of a serrated structure on the inner side of P5 and from *Neocalanus* by the lack of a curved spine near the outer spine of the first exopodite of P2 (Bradford-Grieve et al., 1999). Three species of the *Calanoides* genus are distributed in the coastal waters of Antarctica. Due to the broken P5s of the individual, clear characterisation of the species could not be achieved. However, in *C. acutus*, the long A1 extending beyond the caudal rami is one of the distinguishing features of this species (Bradford-Grieve et al., 1999). In our current species, A1 was also observed to extend slightly beyond the caudal rami (Figure 4b). In molecular analyses, the similarity ratio of copepodites belonging to this genus with *C. acutus* varied between 87.92% and 99.66%.

*Calanoides acutus* is quite common in the coastal waters of Antarctica and contributes significantly to Copepoda biomass. Its contribution to Copepoda abundance has been observed to be 3.2% in surface waters (Pinkerton et al., 2020). The widespread distribution of this species has also been confirmed in studies conducted in Naumayer Channel and on Galindez Island (Yılmaz et al., 2018). This herbivorous

species (Smith and Schnack-Shiel, 1990) has adapted to living in the high primary production waters of the Southern Ocean. *C. acutus* exhibits a distinct seasonal cycle, migrating to the surface in early spring when phytoplankton abundance increases, and then descending to deeper waters again in autumn for overwintering (Smith and Schnack-Shiel, 1990).

In individuals of the genus *Ctenocalanus*, detailed examination could not be performed due to the broken condition of the P2-P4 legs. *Ctenocalanus* species can be easily distinguished from other individuals in the *Clausocalanidae* family by the comb-like structure of the exopods in P3 and P4 (Bradford-Grieve et al., 1999). However, the P5 morphology of female and male individuals, as well as the basis morphology of P2 and P3 in males, confirmed their belonging to the *Ctenocalanus* genus. Specifically, the male *Ctenocalanus* individual is differentiated from the *Farrania* genus by having a single-branched P5, from the *Drepanopus* genus by the long side of P5 having five segments, and from the *Clausocalanus* genus by the fifth segment of P5 being apically attached to the fourth segment (Bradford-Grieve et al., 1999). Due to the broken condition of A1 in females and the exopodites and endopodites of the P2-P4 legs, species-level identification could not be made. Molecular analyses also did not yield successful

DNA isolation results. To date, only one individual of the genus *Ctenocalanus* (*Ctenocalanus vanus*) has been observed in the coastal waters of the Antarctic zone (Razaouls et al., 2005-2022). In the Sub-Antarctic zone, the presence of *C. citer* alongside *Ctenocalanus vanus* is known (Razaouls et al., 2005-2022). Although many characteristic structures of the individuals we examined are damaged, their body and P5 structures exhibit a morphology closer to *C. citer*. Additionally, *C. citer* is one of the dominant species in the Copepoda community, and T. Park's personal observations have indicated that several records reported as *C. vanus* in the Subarctic region were actually *C. citer* (Park and Ferrari, 2008). *C. citer* constitutes 27% of the Copepoda in the surface waters of the Southern Hemisphere oceans. The *Calanoida* species identified as *Ctenocalanus sp.* is similarly the most commonly found Copepoda species in our sampling area. Although only one *Ctenocalanus* species has been reported in this region in terms of ecological distribution, there are no morphological or molecular results to confirm that these individuals are *C. citer*. Therefore, it has been deemed appropriate to identify them as *Ctenocalanus*

Three species of the genus *Paralabidocera* are distributed in the coastal waters of Antarctica (Razaoul et al., 2005-2022). DNA isolation could not be performed from female individuals, and molecular characterization was carried out on a male specimen. The molecular analysis revealed that the individual is *P. grandipina* (98.34%). Female *P. grandipina* are distinguished from the other two species by the structure of their genital segment. Although the body of the female specimen in the samples is deformed, making it not very distinct, the presence of a single protrusion on the left side of the genital segment allows for morphological differentiation from other species (Waghorn, 1975). In *Paralabidocera antartica*, there are four symmetrical lobes, two on each side. In *Paralabidocera separabilis*, the genital segment is almost symmetrical and lacks lobes (Waghorn, 1975). The morphology of the P5 in the individual resembles that of *P. antartica*. Waghorn (1975) did not provide detailed information on the P5 morphology of female individuals when describing the species. Therefore, based on the drawing, it was noted that the P5 segments of the specimen are longer, and the lobes of the forked structure at the distal end are also longer and more pronounced. This resembles the female P5 morphology in *P. antartica*. Furthermore, although the genital segment is deformed, it is evident that the individual possesses a single lobe. In male *P. grandipina*, a small lobed seta within the first segment of the right leg is not very pronounced in our specimen. Additionally, the angular protrusion in the second segment is absent in our individual (Figure 3.l). The seta on the terminal segment of the right leg in *P. grandipina* is long and has given the species its name. However, in our specimen, this seta is small, similar to that of *P. antartica*. Due to the presence of only a single individual and its use in molecular analyses, detailed morphological

characterization could not be conducted. Since there are no comprehensive morphological studies related to this species, intra-species variations are not well understood. The distribution of *Paralabidocera* species is limited to the Sub-Antarctic and Antarctic regions in the Southern Hemisphere (Razaoul et al., 2005-2022). *P. grandipina* is one of the rare Copepoda species, found only in the Pacific sector of Antarctica, and is considered an endemic species of the region. The distribution of *P. antartica* has been reported in many sources, known to occur in the Atlantic and Indian Ocean sectors of Antarctica, including the South Shetland Islands and in the southernmost regions of the Ross Sea. *Paralabidocera separabilis* is also a rare species, distributed in the Indian Ocean sector (Park and Ferrari, 2008). More detailed studies are needed on the molecular and morphological characteristics of this species.

A total of five species of the genus *Oithona* are distributed along the coasts of Antarctica (Razaoul et al., 2005-2022; Yılmaz et al., 2018). Among these species, two have been identified through morphological studies. The same samples were also used for molecular analyses; however, due to the small number of individuals, DNA isolation could not be performed. In the *Oithona similis* group, the distal end of the cephalosome appears blunt when viewed dorsally, while the pointed rostrum is easily visible from the lateral view (Bradford-Grieve, 1999). This head structure allows for easy differentiation from other species found in the region. Its body structure is finer compared to other species. Additionally, the leg seta formula and the absence of setae on the endopod of Mx1 are distinctive features of this species (Bradford-Grieve, 1999). It has a similar morphological structure to *Oithona decipiens* and *Oithona fallax*, which do not occur along the Antarctic coasts. *O. fallax* can be distinguished by the presence of Li2 and Le1 in Mx2, while *O. decipiens* is characterized by the absence of setae on the outer side of the second exopodite of P2 (Bradford-Grieve, 1999). *O. frigida* shows a distinctly pointed rostrum at the distal end of the head when viewed dorsally, similar to *Oithona plumifera* and *Oithona atlantica* observed along the Antarctic coasts (Bradford-Grieve, 1999). When viewed laterally, it has a slightly curved structure pointing forward. However, *O. frigida* can be easily distinguished from these species through its leg seta formula (Bradford-Grieve, 1999). While the P2 exopodites of other species have two setae on the third segment, *O. frigida* has three setae (Bradford-Grieve, 1999). *O. frigida* shares a very similar morphological structure with *Oithona pseudofrigida*, but can be easily differentiated from it by the absence of setae on the inner side of the first exopodites of P2-P4 and the presence of two undeveloped spinules on the outer edge of the P3 exopodite (Bradford-Grieve, 1999).

*Oithona similis* is a cosmopolitan species that has a widespread distribution worldwide (Razaoul et al., 2005-2022). It is one of the species that also shows a highly

widespread distribution along the coasts and open waters of Antarctica, constituting approximately 97% of Cyclopoida (Pinkerton et al., 2020). Previous studies in the region have identified this species as one of the most common and abundant copepod species (Yılmaz et al., 2018). *O. frigida*, on the other hand, is limited to the Southern Hemisphere and is endemic (Razaoul et al., 2005-2022).

The degradation of DNA in certain samples, likely due to the inability to maintain laboratory conditions and the prolonged exposure to polar travel conditions, has posed some challenges for DNA barcoding procedures. However, the results of DNA barcoding conducted on samples with intact DNA have shown a 100% concordance with the morphological characterization results. This demonstrates that DNA barcoding technology is an extremely suitable complementary method for morphological characterization.

## Conclusions

This study provides a comprehensive morphological and molecular analysis of several zooplankton species from Antarctic waters, focusing on *Calanoides acutus*, *Paralabidocera grandispina*, and members of the Oithona genus. Key findings include: Morphological Limitations, Species Identification Challenges. Distribution Insights Genus-specific Characteristics, Diversity of the Oithona Genus and Recommendations for Future Research. Overall, this study highlights both the complexity and the significance of copepod diversity in Antarctic marine ecosystems, while also identifying critical areas for further research to enhance understanding and conservation efforts.

## Ethical Statement

The study does not require approval from a local ethics committee.

## Funding Information

## Author Contribution

A.K and Y.Y. conceived and designed the study, T.T.K and A.K conducted morphological charecterization, Y.Y., M.A.Y., E.V, E.K, H.İ., R.A., M.K conducted laboratory experiments. Y.Y. and A.K. reviewed the manuscript.

## Conflict of Interest

The authors declare no competing interests.

## Acknowledgements

## References

Ashjian, C. J., Rosenwaks, G. A., Wiebe, P. H., Davis, C. S., Gallager, S. M., Copley, N. J., Lawson, G. L., & Alatalo, P. (2004) Distribution of zooplankton on the continental shelf off Marguerite Bay, Antarctic Peninsula, during Austral Fall and Winter, 2001. Deep Sea Research Part II Topical Studies in Oceanography, 51(17–19), 2073–2098. https://doi.org/10.1016/j.dsr2.2004.07.025

Atkinson, A., & Peck, J. M. (1988) A summer-winter comparison of zooplankton in the oceanic area around South Georgia. Polar Biology, 8(6), 463–473. https://doi.org/10.1007/bf00264723

Bardford-Grive, J. M., Markhaseva, E. L., Rocha, C. E. F., & Abiahy, B. (1999) Copepoda, In: South Atlantic. Zooplankton Vol. 2 (Boltovskoy, D., ed.) Backhuys Publishers, Leiden. pp. 869-1097.

Bax, N., Sands, C. J., Gogarty, B., Downey, R. V., Moreau, C. V. E., Moreno, B., Held, C., Paulsen, M. L., McGee, J., Haward, M., & Barnes, D. K. A. (2020) Perspective: Increasing blue carbon around Antarctica is an ecosystem service of considerable societal and economic value worth protecting. Global Change Biology, 27(1), 5–12. https://doi.org/10.1111/gcb.15392

Blanco-Bercial, L., Cornils, A., Copley, N., & Bucklin, A. (2014) DNA barcoding of marine copepods: Assessment of analytical approaches to species identification. PLoS Currents. https://doi.org/10.1371/currents.tol.cdf8b74-881f87e3b01d56b43791626d2

Bucklin, A., Ortman, B. D., Jennings, R. M., Nigro, L. M., Sweetman, C. J., & Copley, N. J. (2010) A "Rosetta Stone" for metazoan zooplankton: DNA barcode analysis of species diversity of the Sargasso Sea (Northwest Atlantic Ocean). Deep-Sea Research Part II, 57, 2234–2247.

Bucklin, A., Steinke, D., & Blanco-Bercial, L. (2011) DNA barcoding of marine metazoa. Annual Review of Marine Science, 3, 471–508.

Chakraborty, M., & Ghosh, S. K. (2014) An assessment of the DNA barcodes of Indian freshwater fishes. Mitochondrial DNA, 537(1), 20–28.

DeSalle, R., Egan, M. G., & Siddall, M. (2005) The unholy trinity: taxonomy, species delimitation and DNA barcoding. Philosophical Transactions of the Royal Society of London. Series B, Biological Sciences, 360(1462), 1905–1916.

Dewitt, H. H., & Hopkins, T. L. (1977) Aspects of the diet of the Antarctic silverfish Pleuragramma antarcticum. In: Proceedings of the 3rd SCAR Symposium of Antarctic Biology. Smithsonian Institute Publishers, pp. 557-567.

Dietrich, K. S., Santora, J. A., & Reiss, C. S. (2021) Winter and summer biogeography of macrozooplankton community structure in the northern Antarctic Peninsula ecosystem. Progress in Oceanography, 196, 102610. https://doi.org/10.1016/j.pocean.2021.102610

Folmer, O., Black, M., Hoeh, W., Lutz, R., & Vrijenhoek, R. (1994) DNA primers for amplification of mitochondrial cytochrome c oxidase subunit I from diverse metazoan invertebrates. Molecular Marine Biology and Biotechnology, 3(5), 294–299.

Geller, J., Meyer, C., Parker, M., & Hawk, H. (2013) Redesign of PCR primers for mitochondrial cytochrome c oxidase subunit I for marine invertebrates and application in all-taxa biotic surveys. Molecular Ecology Resources, 13(5), 851–861.

Goodall-Copestake, W. P., Pérez-Espona, S., Clark, M. S., Murphy, E. J., Seear, P. J., & Tarling, G. A. (2010) Swarms of diversity at the gene cox1 in Antarctic krill. Heredity, 104(5), 513–518.

Gorelova, T. A., & Gerasimchook, V. V. (1981) Data on nutrition and daily consumption of juvenile Pleuragramma antarcticum Boutenger. In: Fishes of the Open Ocean, Academy of Sciences of the USSR Publishers, 103-109

Hebert, P. D. N., & Gregory, T. R. (2005) The promise of DNA barcoding for taxonomy. Systematic Biology, 54(5), 852–859.

Hebert, P. D. N., Ratnasingham S, & Waard J. (2003) Barcoding animal life: cytochrome c oxidase subunit 1 divergences among closely related species. Proc. R. Soc. Lond. B., 270, 96–S99.

Hebert, P. D. N., Ratnasingham, S., & Waard, J. (2003) Barcoding animal life: cytochrome c oxidase subunit 1 divergences among closely related species. Proceedings of the Royal Society of London B, 270, 96–S99.

Heneghan, R. F., Everett, J. D., Blanchard, J. L., & Richardson, A. J. (2016) Zooplankton are not fish: Improving zooplankton realism in size-spectrum models mediates energy transfer in food webs. Frontiers in Marine Science, 3. https://doi.org/10.3389/fmars.2016.00201

Hernando, M., Varela, D. E., Malanga, G., Almandoz, G. O., & Schloss, I. R. (2020) Effects of climate-induced changes in temperature and salinity on phytoplankton physiology and stress responses in coastal Antarctica. Journal of Experimental Marine Biology and Ecology, 530–531, 151400. https://doi.org/10.1016/j.jembe.2020.151400

Hopkins, T. L., Lancraft, T. M., Torres, J. J., & Donnelly, J. (1993) Community structure and trophic ecology of zooplankton in the Scotia Sea marginal ice zone in winter (1988). Deep Sea Research Part I Oceanographic Research Papers, 40(1), 81–105. https://doi.org/10.1016/0967-0637(93)90054-7

Hubold, G. (1985) The early life-history of the high-Antarctic silverfish, Pleuragramma antarcticum. In Springer eBooks (pp. 445–451). https://doi.org/10.1007/978-3-642-82275-9_62

Hunt, B., Pakhomov, E., Siegel, V., Strass, V., Cisewski, B., & Bathmann, U. (2010) The seasonal cycle of the Lazarev Sea macrozooplankton community and a potential shift to top-down trophic control in winter. Deep Sea Research Part II Topical Studies in Oceanography, 58(13–16), 1662–1676. https://doi.org/10.1016/j.dsr2.2010.11.016

Johnson, C. L., Runge, J. A., Curtis, K. A., Durbin, E. G., Hare, J. A., Incze, L. S., Link, J. S., Melvin, G. D., O'Brien, T. D., & Van Guelpen, L. (2011) Biodiversity and ecosystem function in the Gulf of Maine: Pattern and role of zooplankton and pelagic nekton. PLoS ONE, 6(1), e16491. https://doi.org/10.1371/journal.pone.0016491

Krupnik, I., Lang, M. A., & Miller, S. E. (2009) Species diversity and distributions of pelagic calanoid copepods (Crustacea) from the Southern Ocean. https://repository.si.edu/handle/10088/6820

Lancraft, T., Hopkins, T., Torres, J., & Donnelly, J. (1991) Oceanic micronektonic/macrozooplanktonic community structure and feeding in ice-covered Antarctic waters during the winter (AMERIEZ 1988). Polar Biology, 11(3). https://doi.org/10.1007/bf00240204

Lee, J. R., Raymond, B., Bracegirdle, T. J., Chadès, I., Fuller, R. A., Shaw, J. D., & Terauds, A. (2017) Climate change drives expansion of Antarctic ice-free habitat. Nature, 547(7661), 49–54. https://doi.org/10.1038/nature22996

Machida, R. J., Miya, M. U., Nishida, M., & Nishida, S. (2004) Large-scale gene rearrangements in the mitochondrial genomes of two calanoid copepods Eucalanus bungii and Neocalanus cristatus (Crustacea), with notes on new versatile primers for the srRNA and COI genes. Gene, 332, 71–78. PMID: 15145056.

Nordhausen, W. (1994) Winter abundance and distribution of Euphausia superba, E. crystallorophias, and Thysanoessa macrura in Gerlache Strait and Crystal Sound, Antarctica. Marine Ecology Progress Series, 109, 131–131.

Pakhomov, E. A., & Pankratov, S. A. (1992) Feeding of juvenile notothenioid fishes of the Indian sector of the Antarctic. Journal of Ichthyology, 32, 28–37.

Park, E. T., & Ferrari, F. D. (2009). Species diversity and distributions of pelagic calanoid copepods (Crustacea) from the Southern Ocean. Smithsonian at the poles: contributions to international polar year science.

Pinkerton, M. H., Décima, M., Kitchener, J. A., Takahashi, K. T., Robinson, K. V., Stewart, R., & Hosie, G. W. (2020) Zooplankton in the Southern Ocean from the continuous plankton recorder: Distributions and long-term change. Deep Sea Research Part I: Oceanographic Research Papers, 162, 103303.

Ratnarajah, L., Abu-Alhaija, R., Atkinson, A., Batten, S., Bax, N. J., Bernard, K. S., & Yebra, L. (2023) Monitoring and modelling marine zooplankton in a changing climate. Nature Communications, 14(1), 564.

Razouls, C., Desreumaux, N., Kouwenberg, J., & de Bovée, F. (2005-2022) Biodiversity of marine planktonic copepods (morphology, geographical distribution and biological data). Sorbonne University, CNRS. Available at http://copepodes.obs-banyuls.fr/en

Reid, K., Croxall, J. P., Briggs, D., & Murphy, E. (2005) Antarctic ecosystem monitoring: Quantifying the response of ecosystem indicators to variability in Antarctic krill. ICES Journal of Marine Science, 62, 366–373.

Richon, C., & Tagliabue, A. (2021) Biogeochemical feedbacks associated with the response of micronutrient recycling by zooplankton to climate change. Global Change Biology, 27(19), 4758–4770.

Schwarzbach, W. (1988) Die Fischfauna des östlichen und südlichen Weddellmeeres geographische Verbreitung, Nahrung und trophische Stellung der Fischarten. Berichte Polarforschung, 54, 1–94.

Simonsen, K. A., Ressler, P. H., Rooper, C. N., & Zador, S. G. (2016) Spatio-temporal distribution of euphausiids: An important component to understanding ecosystem processes in the Gulf of Alaska and eastern Bering Sea. ICES Journal of Marine Science, 73(8), 2020–2036.

Waghorn, E. J. (1979) Two new species of Copepoda from White Island, Antarctica. New Zealand Journal of Marine & Freshwater Research, 13(3), 459–470.

Ward, P., Grant, S., & Brandon, M. (2004) Mesozooplankton community structure in the Scotia Sea during the

CCAMLR 2000 Survey: January-February 2000. Deep-Sea Research Part II, 51(12-13), 1351–136.

Williams, R. (1985) Trophic relationships between pelagic fish and euphausiids in Antarctic waters. In: Antarctic Nutrient Cycles and Food Webs. Springer-Verlag, 452–459.

Yang, G., Li, C. L., & Sun, S. (2011) Inter-annual variation in summer zooplankton community structure in Prydz Bay, Antarctica, from 1999 to 2006. Polar Biology, 34(6), 921–932.

Yilmaz, I. N., Ergul, H. A., Mavruk, S., Tas, S., Aker, H. V., Yildiz, M., & Ozturk, B. (2018) Coastal plankton assemblages in the vicinity of Galindez Island and Neumayer Channel (Western Antarctic Peninsula) during the first joint Turkish-Ukrainian Antarctic research expedition. Turkish Journal of Fisheries and Aquatic Sciences, 18, 577–584.